Design of Asymmetric CPW Fed Bow-tie Slot Antenna For WLAN/WiMax Systems

M.Sunnybabu[1] *K.Venkatesulu*[2] *V.Srinivas*[3]

[1]*P.G.Scholar, Department of ECE, Swarnandhra Institute of Engineering Technology, Narasapuram, Andhra Pradesh*
[2, 3] *Department of ECE, Swarnandhra Institute of Engineering Technology, Narasapuram, Andhra Pradesh*
sunnybabu.m99@gmail.com

Abstract— With the rapid developments in wireless communication technology, higher requirements are put forward to antenna system. Wideband and compact antennas are required by satellite communications system, and personal communications system. Bow-tie slot antennas with wide bandwidth and compact structure have received widespread attention. Due to the rapid development of high speed wireless communication, there is an increasing demand for antennas with broadband operation and uniform radiation pattern in the horizontal plane which enables the wireless communication systems owing to its large signal coverage. Here, a new style of broadband bow-tie slot antenna is presented. It is fed by an asymmetric coplanar waveguide (ACPW) with different slot lengths. By adjusting the length of one ACPW slot, the impedance characteristic of the antenna is greatly improved so that the bandwidth is broadened. The proposed antenna topology is characterized by its small size compared to conventional bow-tie antennas it is constructed from two right angle triangle slots, with round corners. It cover the WLAN (2.4 GHz, 3.65 GHz) and WiMax (2.3 GHz, 2.5 GHz, and 3.5 GHz) spectra.

Index Terms— **Omni directional antennas, slot antennas, flexible antennas, bow-tie, coplanar waveguides.**

I. INTRODUCTION

PRINTED slot antennas have numerous appealing characteristics making them attractive for wireless communications [1-8]. Compared to micro strip antennas , they have wider bandwidth , better matching, and are capable of radiating either uni-directional or bi-directional [1-3]. Slot bow-tie antennas, one example of slot antennas, received great attention due to their capability of providing wide bandwidth. Several approaches were implemented to further enhance the bandwidth of these antennas and/or to make them suitable for multi-band operation. In [4], two small metal sectors are placed inside the slot of a bow-tie antenna to increase its bandwidth. In [5], the effect of round corners on the performance of bow-tie antennas is studied. It was demonstrated that rounding the corners enhances the return loss, flattens the input impedance, and stabilizes the radiation pattern. In [6], [7], tuning stubs are added for dual band [6] or triple band [7] applications.

Recently, flexible technologies witnessed great progress for lots of applications including flexible displays, health monitoring systems, and flexible sensors [9]. As traditional planar antennas that are fabricated from classical rigid materials, flexible antennas can be designed with light weight, small thickness, and low profile [9]. Furthermore, they can be easily mounted on conformal surfaces. Textile antennas [10, 11], paper-based antennas [12,13], and synthesized flexible substrates [14,15], all are examples of flexible antennas. In [10], a dual-band E-shape antenna operating at 2.2 GHz and 3 GHz was presented. The antenna is fabricated on felt fabric making it suitable for wearable applications. However, textile materials are likely subjected to discontinuities and fluids absorption. In [12], a single band antenna which is fabricated on a paper substrate was introduced. The antenna operates at 2.5 GHz which is suitable for Wireless Local Area Network (WLAN) applications. Nevertheless, paper has relatively high losses as a result from its dielectric loss tangent (tan δ) = 0.07 at 2.45 GHz.

Additionally, for applications requiring high bending and rolling, paper substrates are not recommended as they are not robust and might introduce discontinuities. Other substrates are also considered in the literature including heat stabilized polyethylene naphthalate [14], flexible parlyne [15], organic substrate [16], and polyethylene terephthalate (PET) [17-19]. In this communication, we present two versions of a flexible wideband slot bow-tie antenna with round corners. The first case corresponds to a bow-tie antenna in free-space while the second one takes into consideration the presence of a brick wall as a supporting surface for the bow-tie antenna. The proposed antenna topology is characterized by its small size compared to conventional bow-tie antennas.

The antenna radiates omnidirectionally and is characterized by its good matching all over the frequency range from 2.2 GHz to at least 3.7 GHz, making it suitable for WLAN/WiMax systems.

Table 1 summarizes a comparison between the proposed antenna with other bow-tie antennas presented in the literature. As shown,the proposed antenna has the highest gain compared to [4, 6 and 8]. Meanwhile, its bandwidth is less than [4] but higher than [6, and 7]. The communication is organized as follows. The structure of the proposed antenna is presented in Section II.

A parametric study is performed in Section III while the effect of adding a supporting surface underneath the antenna is highlighted in section IV.

The experimental characterization of the fabricated prototype along with explanation of the radiation mechanism is presented in Section V. The main conclusions are stated in Section VI.

II. STRUCTURE OF THE BOW-TIE SLOT ANTENNA

Fig. 1 shows the structure of the proposed bow-tie antenna. The antenna is fabricated on top of 0.2 mm thick flexible Rogers RO4003C substrate (r □ = 3.38 and tan δ = 0.0027) covered with 17 □m copper from one side. The overall size of the proposed antenna is 80 mm □ 60 mm. The bow-tie antenna is constructed from two right angle triangle slots, with round corners, as shown in Fig. 1. The outside corners are rounded with radius equals to the slot width in order to reduce the overall size of the antenna. The length of the triangle's arm perpendicular to the feeding line is *L*. This arm forms an angle of ca. 60˚□70˚ with the hypotenuse arm, as shown in Fig. 1, which promotes close-enough arm resonances, in order to get a wide band. All arms of the triangles have the same slot width, denoted by *W*.

The antenna is fed by a coplanar waveguide (CPW) transmission line of 50 Ω characteristic impedance. The length, width and spacing of the CPW's slots are 14.03 mm, 0.25 mm and 5.75 mm, respectively. A quarter-wavelength transformer designed at 3 GHz is inserted between the antenna and the CPW feeding line. It is worth mentioning that the proposed antenna could be seen as a half bow-tie antenna; thus, it has smaller size compared to conventional bow-tie antennas. The radiating slot triangles of the bow-tie are oriented in the same direction of the transmission line to assure a minimum size for the antenna.

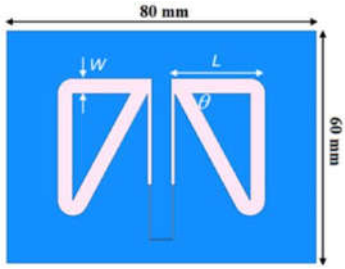

Fig. 1. Structure of the proposed CPW-fed bow-tie slot antenna. The dark (light) area represents the copper layer (slot locations in the copper layer).

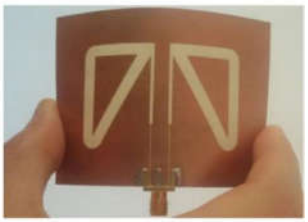

Fig.2. The fabricated flexible bow-tie antenna

TABLE I
COMPARISON BETWEEN FLEXIBLE ANTENNAS PRESENTED IN THE LITERATURE

Ref.	Size	Max Gain	Bandwidth
[4]	30 mmx26mm	--	12.9 GHz (80%)*
[6]	60 mmx45 mm	3.65 dBi	1.94 GHz (32.33%)
[7]	35 mmx35 mm	1.36 dBi	1.405 GHz (46.56%)
This work	80 mmx60 mm	6.20 dBi*	1.79 GHz (57.7%)

It should be mentioned here that the supporting surface is expected to interact with the near-field of the antenna as the substrate is very thin electrically. Hence, the dimensions of the antenna should be retuned according to the dielectric properties of the supporting surface. That is why in this work, two versions of the bow-tie antenna are considered, representing the two "extremes". The first antenna is designed to operate in free-space, while the second one is mounted on top of a brick wall supporting surface. The exact angle is 60˚ for the first antenna and 70.6˚ for the second one. The length, width and spacing of the transformer's slots for the first (second) antenna version antenna are L_{trans}= 25.5 mm (16.65 mm), W_{trans}= 1.1 mm (1.35 mm) and S_{trans}= 4.9 mm (4.5 mm), respectively. The approach to tune the proposed antenna is outlined in Section IV.

The antenna is excited via the odd mode of the CPW line. Therefore, magnetic currents flow along the two slots of the CPW in opposite directions. Magnetic currents then flow along the two slotted triangles at both sides of the CPW. Due to the odd symmetry of the feeding magnetic currents, the horizontal magnetic current components, which are orthogonal to the feeding slots, add constructively to each other. On the other hand, radiation from vertical magnetic current components along the two triangles forming the bow-tie cancels out along the *y*-axis. The detailed explanation of the radiation mechanism of the proposed antenna is presented in Section V. Fig. 2 shows the fabricated bow-tie antenna in free-space. Standard printed circuit board (PCB) technology is used for fabrication. It is clear from the figure that the antenna is flexible enough to be mounted on any supporting surface.

III PARAMETRIC STUDY

In this section, the effect of varying the main geometrical parameters of the bow-tie antenna on its frequency response is studied. The bow-tie antenna in free-space is considered in this study. Fig. 3 shows the reflection coefficient versus frequency at different values of *L*. As *L* increases, the first (lowest) and third (highest) resonances shift to lower frequencies, while the second (middle) resonance frequency is almost unchanged. This is due to the fact that increasing *L* implies the increase of the lengths of all the triangles' arms since the angle θ is kept constant. It will be shown in Section V, that the horizontal and diagonal arms are the main radiators of the proposed structure. Therefore, the first and third resonances are attributed to the radiation from the diagonal (longer) and horizontal (shorter) arms, respectively. The middle resonance is due to the pesence of the quarter wavelength transformer inserted between the antenna and the feeding CPW line. Thus, varying the lengths of the antenrna's arms has no effect on the value of the second resonance frequency. In addition to the shift in the locations of the first and third resonances, changing *L* affects the degree of matching between the CPW characteristic impedance and the antenna input impedance, which is dependent on *L*.

Fig. 4 shows the reflection coefficient versus frequency for different values of *W*. It is clear from the figure that as *W* increases, the first and third resonances, which correspond to the diagonal and horizontal arms, respectively, shift to higher frequencies. This can be explained as follows: as *W* increases, the equivalent capacitance, *C*, of the radiating slotline arms decreases leading to a decrease in the propagation constant $\sqrt{C}$. As a result, the effective dielectric constant decreases $\sqrt{\varepsilon_{r,eff}}/C$. Since the radiating arms' lengths are kept constant, and the guided wavelength $\lambda_{g0}/\sqrt{\varepsilon_{r,eff}}$ at resonance satisfies the resonance condition, the decrease in the effective dielectric constant should be compensated by a decrease in the free-space wavelength, which means an increase in the resonance frequency. Similar to its behavior with the variation in *L*, the location of the second resonance is unaffected by the variation in *W*. Only the level of matching at the second resonance is affected by *W*. An intensive parametric study has been performed in order to force the three operating bandwidths around the three resonance frequencies to be slightly overlapping. This results in the widest possible bandwidth. The optimum values of *L* and *W* are found to be 24.45 mm and 4 mm, respectively.

IV. DEMONSTRATION OF TUNABILITY

This section presents a study about the effect of placing the new bow-tie topology on a supporting structure. Specifically, the case of a bow-tie antenna on top of a thick brick wall is considered as it is one of the targeted very practical cases. The dielectric properties of bricks are given by: ε_r 4.86 , tan δ = 0.049 , and thickness of 92 mm [20]. The simulated reflection coefficient versus frequency for the free-space version of the topology but put on the brick wall is shown in Fig. 5. Due to the high dielectric relative permittivity of the brick wall compared to free-space, the bandwidth of the antenna shifts to lower frequencies. Furthermore, the relative locations of the resonating frequencies are changed with respect to each other leading to separating the overlapping bands. The retuning of the topology, resulting in version 2, consists of two simple steps. First, the length of the bow-tie arms should be decreased in order to tune the operational frequency. Second, the quarter wavelength transformer parameters must be modified in order to reconstruct the new matching conditions. After re-tuning the antenna withs the new parameters: *L* = 16.65 mm, L_{trans}= 17.82

Fig.3. S11 of the bow-tie antenna versus frequency for different values of the length *L*. The width, *W*, is kept constant at the optimum value of 4 mm.

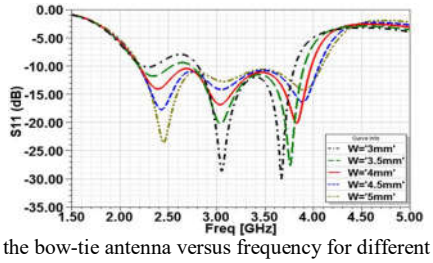

Fig. 4. S11 of the bow-tie antenna versus frequency for different values of the width *W*. The length, *L*, is kept constant at the optimum value of 24.45 mm.

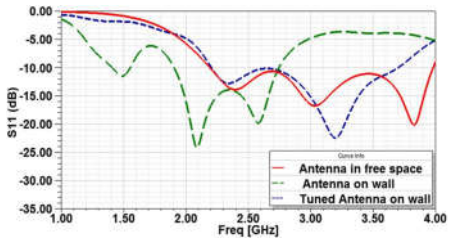

Fig. 5. Reflection coefficient versus frequency for the bow-tie on brick wall.

mm, W_{trans}= 1.35 mm and S_{trans}= 4.5 mm, the reflection coefficient of the antenna on brick-wall is shifted to the desired band as shown in Fig. 5. It is clearly seen that both versions, before and after tuning, cover the entire targeted bandwidth for WLAN and WiMax. Additionally, the size of the antenna is reduced when mounted on this supporting structure. It is worth mentioning that the antenna could be easily retuned for other supporting structures, such as drywall (plasterboard). In this case, the dielectric relative permittivity is $_r$ 2 , which lies
between the relative dielectric permittivity of free-space and that of brick-wall.

V. EXPERIMENTAL CHARACTERIZATION

In this section, the response of the fabricated bow-tie antenna in free-space is measured. Fig. 6 shows the measured and simulated reflection coefficient versus frequency of the fabricated optimum design. As shown, the antenna resonates at 2.4 GHz, 3 GHz, and 3.8 GHz. The operating bandwidths around these resonances are slightly overlapping leading to an overall 10 dB impedance bandwidth as wide as 1.79 GHz, (57.74%). It is evident from Fig. 6 that the measurements and HFSS simulations are in a good agreement. The effect of bending the antenna is shown in Fig. 7. As shown, the bending affects the level of matching, which can be adjusted afterwards by the antenna parameters. It is worth noting that the radiation characteristics of the bent antennas are almost the same for the various simulated radii.

Fig. 6. Measured and simulated S11 of the bow-tie antenna versus frequency.

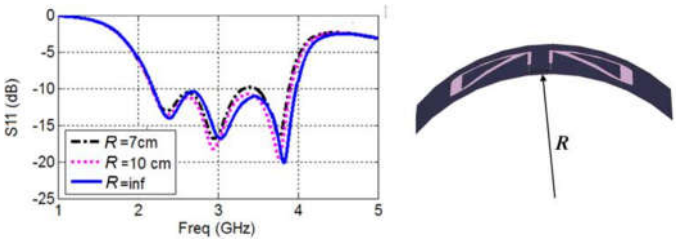

Fig. 7. Effect of bending the bow-tie antenna on its reflection coefficient.

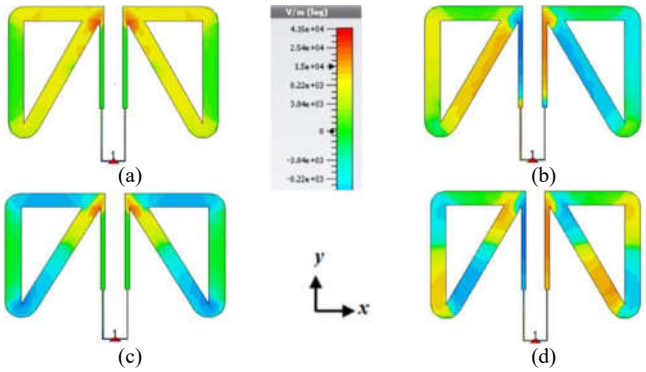

Fig. 8. Electric field distribution along the bow-tie antenna: (a) *x*-(horizontal) component at 2.5 GHz, (b) *y*-(vertical) component at 2.5 GHz, (c) *x*-(horizontal) component at 4 GHz, and (d) *y*-(vertical) component at 4 GHz.

Fig. 8 shows the simulated *x*-(horizontal) and *y*-(vertical) components of the electric field at 2.5 GHz, and 4 GHz. From Fig. 8(a), it is clear that at 2.5 GHz, the *x*-components of the electric field along the horizontal and diagonal arms are in-phase with an even symmetry along the *y*-axis. This means that the radiation resulting from these horizontal and diagonal arms adds up constructively. On the other hand, the *y*-components of the electric field along the bow-tie antenna have odd symmetry around the *y*-axis, as shown in Fig. 8(b). Therefore, radiation resulting from the vertical component of the electric field cancels out along this axis. At 4 GHz, it is clear from Fig. 8(d) that the *y*-components of the electric field of all arms are opposite to each other at both sides of the bow-tie. Hence, this component does not contribute much to the antenna's radiation. The *x*-component, see Fig. 8(c), is very weak along the vertical arms at both sides. This component reverses its direction along each diagonal arm whose length is now greater than half a guided wavelength. Consequently, the contribution of the diagonal arms is negligible. The main radiating arms at 4 GHz are the horizontal arms as the *x*-components of the electric field are strong and in the same direction at both sides of the bow-tie.

Fig. 9 shows the 3D radiation patterns of the bow-tie at 2.5 GHz and 4 GHz, as obtained from HFSS. At both frequencies

the antenna radiates almost omni-directional. The maximum gain calculated using HFSS is 4.30 dBi (6.88 dBi) at 2.5 GHz (4 GHz). The normalized radiation patterns of the bow-tie antenna along the *E*(*yz*)- and *H*(*xz*)- planes are presented in Fig. 10. Good agreement between simulations and measurements at frequencies is observed. The measured broadside cross-polarization levels in the *E*- and *H*- planes are 18.60 dBi (9.44 dBi) and 30.58 dBi (24.40 dBi) at 2.5 GHz (4 GHz). Fig. 11 shows a comparison between the measured and simulated maximum gain versus frequency. Simulations and measurements have similar behavior, as shown in the figure. The measured gain ranges from 2.34 dBi at 2.6 GHz to 6.30 dBi at 3.8 GHz. The measurement setup used to measure the radiation characteristics of the bow-tie antenna is shown in Fig.

12. The calculated radiation efficiency is above 97% all over the working frequency band. Such high value is expected as the substrate is very thin electrically and the copper layer thickness is sufficiently bigger than the skin depth.

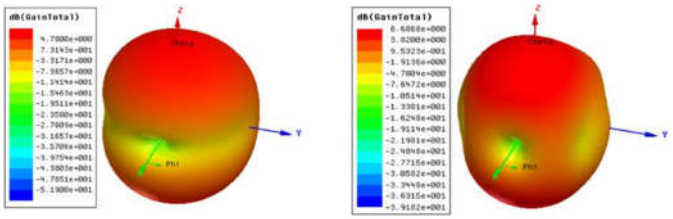

(a) (b)

Fig. 9. 3D radiation patterns for the bow-tie antenna as simulated using HFSS at (a) 2.5 GHz, and (b) 4 GHz.

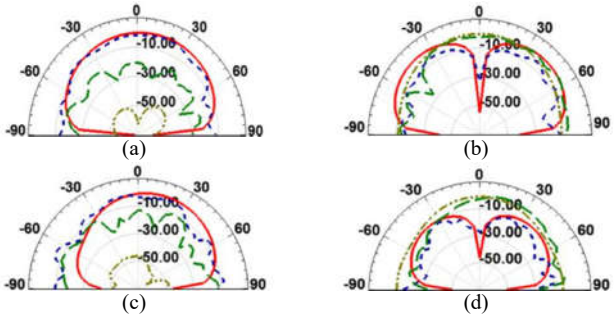

(a) (b) (c) (d)

Fig. 10. Measured and calculated radiation patterns of the bow-tie antenna: (a) *E*(*yz*)- plane at 2.5 GHz, (b) *H*(*xz*)- plane at 2.5 GHz, (c) *E*(*yz*)- plane at 4 GHz, and (d) *H*(*xz*)- plane at 4 GHz. Gain theta (HFSS), Gain theta (measured), Gain phi (HFSS), and Gain phi (measured).

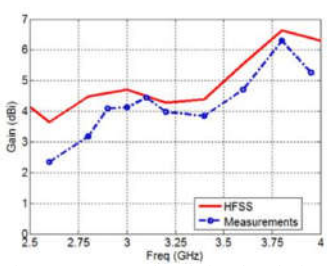

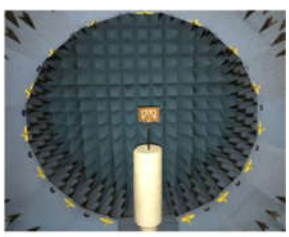

Fig. 11. Measured and simulated gain of the bow-tie antenna setup. Fig. 12. Radiation measurements versus frequency.

VI. CONCLUSION

A new slotted flexible bow-tie antenna is presented. Two versions of the antenna are considered, when placed in free-space and when mounted on top of a brick-wall supporting surface. In both cases, the antenna has overlapping resonances resulting in a wide impedance bandwidth of about 50%. The bow-tie antenna in free-space is fabricated and fully characterized both experimentally and theoretically, which are in good agreement. The antenna radiates bi-directionally with a maximum measured gain of 6.30 dBi occurring at 3.8 GHz.

REFERENCES

[1] J. Yeo, Y. Lee and R. Mittra, "Wideband slot antennas for wireless communications," *IEEE Proc. Microw. Antennas Propag.,* vol.151, no.4, pp.351-355, Aug. 2004.

[2] E. A. Soliman, et al, "Bow-tie slot antenna fed by CPW," *Electron Lett.*, vol.35, no.7, pp.514-515, Apr. 1999.

[3] A. A. Eldek, A. Z. Elsherbeni, and C. E. Smith, "Characteristics of bow-tie slot antenna with tapered tuning stubs for wideband operation," *Progress In Electromagnetics Research*, vol.49, pp.53-69, 2004.

[4] Y.-L. Chen, C.-L. Ruan, and L. Peng, "A novel ultra-wideband bow-tie slot antenna in wireless communication systems," *Progress In Electromagnetics Research,* vol.1, pp.101-108, 2008.

[5] S. W. Qu, and C. L. Ruan, "Effect of round corners on bowtie antennas," *Progress In Electromagnetics Research*, vol.57, pp.179-195, 2006.

[6] L.-C. Tsai, "A dual bow-tie-shaped CPW-fed slot antenna for WLAN applications," *Progress In Electromagnetics Research*, C, vol.47, pp. 167-171, Apr. 2014.

[7] J. H. Yoon, and Y. C. Lee," Modified bow-tie slot antenna for the 2.4/5.2/5.8 GHz WLAN bands with a rectangular tuning stub," *Microw. Opt. Technol. Lett.,* vol.53, no.1, pp.126-130, Jan. 2011.

[8] E. A. Soliman, W. De Raedt, and G. A. E. Vandenbosch, "Reconfigurable slot antenna for polarization diversity," *J. of Electromagn. Waves and Appl.,* vol.23, no.7, pp.905-916, 2009.

[9] H. R. Khaleel, H. M. Al-Rizzo, D. G. Rucker, and Y. Al-Naiemy, "Flexible printed monopole antennas for WLAN applications," ," *IEEE Int. Symp. Antennas Propag. ,* pp.1334-1337, Spokane, WA, Jul. 2011.

[10] P. Salonen, J. Kim, and Y. Rahmat-Sami, "Dual-band E-shaped patch wearable textile antenna," *IEEE Int. Symp. Antennas and Propg. Soc.,* pp.466-469, Jul. 2005.

[11] S. Shao, A. Kiourti, R. J. Burkholder, and J. L. Volakis, "Broadband textile-based passive UHF RFID tag antenna for elastic material," IEEE Antennas and Wireless Propagation Letters, vol.14, 2015.

[12] D. E. Anagnostou, A. A. Gheethan, A. K. Amert, and K. W. Whites, "A direct-write printed antenna on paper-based organic substrate for flexible displays and WLAN applications," *J. of Display Technol.*, vol.6, no.11, pp.558-564, Oct. 2010.

[13] M. Kgwadi, C. J. Vourch, D. J. Harrison, and T. D. Drysdale, "On-demand printing of antennas for TV white-space communications," Antennas and propagation conference (LAPS), pp.553-556, Loughborough, UK, 2014..

[14] H. R. Khaleel, H. M. Al-Rizzo, and A. I. Abbosh, "Design, fabrication, and testing of flexible antennas," *in Advancement in Microstrip Antennas With Recent Applications*, A. Kishk, Ed., InTech, Vienna, Austria, 2013.

[15] B. Tehrani, B. Cook, J. Cooper, M. Tentzeris, "Inkjet printing of a wideband high gain mm-wave vivaldi antenna on a flexible organic substrate," *IEEE Antennas and Propagation International Symposium (APSURSI)*, Memphis, TN. USA, Jul. 2014.

[16] G. A. Casula. G. Montisci, and G. Mazzarella, "A wideband PET inkjet-printed antenna for UHF RFID," *IEEE Antennas and Wireless Propagation Letters*, vol. 12, pp. 1400-1403, 2013.

[17] C. Thajudeen, A. Hoorfar, and F. Ahmad, "Measured complex permittivity of walls with different hydration levels and the effect of power estimation of TWRI target returns," *Progress In Electromagnetics Research* B, vol.30, pp.177-199, 2011.

[18] G. Casula, P. Maxia, A. Fanti, and G. Mazzarella, "A low-cost dual-band CPW-fed printed LPDA for wireless communications," *IEEE Antennnas and Wireless Propagation Letters*, vol. 15, pp.1333-1336, 2016.